The FASEB Journal express article 10.1096/fj.05-3785fje. Published online December 13, 2005.

Targeted calretinin expression in granule cells of calretinin-null mice restores normal cerebellar functions

Bertrand Bearzatto,* Laurent Servais,*,† Céline Roussel,* David Gall,* Fawzia Baba-Aïssa,* Stéphane Schurmans,‡ Alban de Kerchove d'Exaerde,* Guy Cheron,†,§ and Serge N. Schiffmann*

*Laboratory of Neurophysiology, ‡IRIBHM, IBMM, §Laboratory of Movement Biomechanics, Université Libre de Bruxelles, 1070 Brussels, Belgium; †Laboratory of Electrophysiology, Université Mons-Hainaut, 7000 Mons, Belgium

Corresponding author: Serge N. Schiffmann, Laboratory of Neurophysiology, CP601, Université Libre de Bruxelles, route de Lennik 808, 1070 Brussels, Belgium. E-mail: sschiffm@ulb.ac.be

ABSTRACT

Ca^2 binding proteins such as calretinin, characterized by the presence of EF-hand motifs that bind Ca^{2+} ions, are involved in the shaping of intraneuronal Ca^{2+} fluxes. In the cerebellar cortex, information processing tightly relies on variations in intracellular Ca^{2+} concentration in Purkinje and granule cells. Calretinin-deficient ($Cr^{-/-}$) mice present motor discoordination, suggesting cellular and network cerebellar dysfunctions. To determine the cell specificity of these alterations, we constructed transgenic $Cr^{-/-}$ mice exhibiting a selective reexpression of calretinin in granule cells through the promoter function of the $GABA_A$ receptor α6 subunit gene. Normal granule cell excitability and wild-type Purkinje cell firing behavior in awake mice were restored while the emergence of high-frequency oscillations was abolished. Behavioral analysis of these calretinin-rescue mice revealed that normal motor coordination was restored as compared with $Cr^{-/-}$ mice. These results demonstrate that calretinin is required specifically in granule cells for correct computation in the cerebellar cortex and indicate that the finetuning of granule cell excitability through regulation of Ca^{2+} homeostasis plays a crucial role for information coding and storage in the cerebellum.

Key words: calcium binding protein • cerebellum • targeted gene expression • calcium homeostasis • $GABA_A$-α6

Intracellular calcium concentration ($[Ca^{2+}]i$) is tightly controlled via the regulatory system of Ca^{2+} homeostasis, which consists of Ca^{2+} entry systems (e.g., channels), intracellular compartments involved in Ca^{2+} release and uptake (sarco/endoplasmic reticulum, mitochondria), Ca^{2+} extrusion mechanisms, and Ca^{2+} buffers, including calcium binding proteins (1). These latter, which are characterized by EF-hand motifs that bind calcium with high affinity, play a key role in the regulation of $[Ca^{2+}]i$, leading to specific adjustments of neuronal signaling. Variations in $[Ca^{2+}]i$ play a crucial role in information processing in the cerebellar cortex, both in Purkinje (2) and granule cells as they modulate the efficacy of both excitatory and inhibitory inputs (3–5) and are involved in the induction of synaptic plasticity (3, 6, 7). Among calcium

binding proteins, calretinin is the main one to be expressed in cerebellar granule cells (8, 9), whereas the structurally related calbindin is exclusively expressed in Purkinje cells.

Granule cells process information entering into the cerebellar cortex through the mossy fibers, the largest cerebellar afferent system originating from various regions in the spinal cord, brainstem, and cerebral cortex. They convey the major excitatory afference to Purkinje cells through the parallel fibers. We previously showed that calretinin-deficient mice ($Cr^{-/-}$) present motor discoordination, suggesting cerebellar dysfunction (10). They also display alterations in Purkinje cell firing recorded in vivo under the form of an increase in simple spike firing rate and a decrease in the complex spike and subsequent pause duration (10). Moreover, patch-clamp recordings on brain slices showed that granule cells of $Cr^{-/-}$ mice exhibit an altered intrinsic neuronal excitability that is directly linked to the decrease in Ca^{2+} buffering capacity (11), whereas Purkinje cells have normal intrinsic properties (10). Finally, recordings in alert $Cr^{-/-}$ mice also revealed the induction of a fast network oscillation that was not observed in wild-type (WT) mice (12). Thus, calretinin is thought to be essential for correct computation in the cerebellar cortex and, hence, for the maintenance of an adequate cerebellar physiology.

However, calretinin is also expressed in various cell types in the central nervous system other than granule cells, both outside and inside the cerebellum. In the cerebellar cortex, calretinin is expressed in subsets of mossy and climbing fibers and in interneurons such as unipolar brush cells (UBCs) and Lugaro cells (8, 9, 13, 14). Therefore, it is not clear to what extent calretinin in granule cells contributes to the phenotypes detected in $Cr^{-/-}$ mice. To address that question, we have generated $Cr^{-/-}$ mice that selectively reexpress calretinin in granule cells (hereafter referred to as Cr-rescue mice) through the promoter function of a fragment of the gene coding for the $GABA_A$ receptor α6 subunit ($GABA_A$-α6) (15). Our results show that the rescued expression of calretinin in granule cells of $Cr^{-/-}$ mice restores normal cerebellar physiology and motor coordination.

MATERIALS AND METHODS

Transgene construction

Mouse calretinin cDNA was cloned by RT-PCR from mouse brain mRNA library using the following primers: forward, 5′-ACA ACT AGT CCA TGG CTG GCC CGC AGC A-3′; reverse, 5′-ATT GGA TCC CTG TCC CTT CAC CCC TTT-3′. The forward primer was designed to add the Spe I-Nco I restrictions sites and the reverse primer to add a Bam HI restriction site to calretinin cDNA.

The simian virus 40 polyadenylation sequence (poly A) was isolated from pSG5 (Stratagene, La Jolla, CA) by Eco RI-Sal I digestion and inserted in a pBluescript vector (Stratagene). After digestion, the Spe I-Bam HI calretinin cDNA was inserted in pBluescript containing the SV40 poly A to yield: p-calretinin-polyA.

The 7.85 kb SphI(blunded)-NcoI fragment from the pmα6IRES-LacZ6 vector (15) (containing 1 kb sequence located upstream of the transcription start site, exons 1-8 of the $GABA_A$-α6 and an internal ribosome entry site [IRES]) was isolated. This fragment was then ligated in the SpeI (blunded)-NcoI p-calretinin-polyA to yield the final construction pmα6IRES-calretinin-polyA (Fig. 1*A*).

Generation of transgenic mice

Transgenic mice were generated by microinjection of the transgene into oocytes from superovulated C57Bl6 × SJL mice. Transgenic mice were screened by PCR on DNA extracted from tail biopsies. The 5′-oligonucleotide primer sequence was from IRES sequence (IRES I: 5′-CGT CTG TAG CGA CCC TTT GCA GGC AGC-3′), and the 3′ reverse primer sequence was from the calretinin cDNA sequence (CS II: 5′-CCA GAA CCC TTC CTT GCC TTC TCC AGC-3′) (Fig. 1A). PCR conditions were 94°C for 3 min, then 35 cycle at 94°C for 30 s, 65°C for 45 s and 72°C for 1 min, followed by 72°C for 10 min. The founders (C57Bl6 × SJL) were first crossed with C57Bl6 calretinin knockout mice (F7) (11) to obtain F1 $Cr^{+/-}$ Tg^{+} mice. These animals were then crossed two times either with C57Bl6 $Cr^{-/-}$ mice or C57Bl6 WT mice to finally obtain F3 $Cr^{-/-}$ Tg^{+}, F3 $Cr^{-/-}$ Tg^{-}, and F3 $Cr^{+/+}$ Tg^{-} mice. If not otherwise mentioned, all analyses were done on these F3 littermates, including Cr-rescue $Cr^{-/-}$ Tg^{+}, knockout $Cr^{-/-}$ Tg^{-}, and WT $Cr^{+/+}$ Tg^{-} mice with the same genetic background (theoretically 93.75% C57Bl6 and 6.25% SJL). For the behavioral analysis, we restored the original hybrid background (see Results). Animals were crossed two more times with C57Bl6 $Cr^{-/-}$ mice to finally obtain F5 $Cr^{-/-}$ Tg^{+} (theoretically 98.44% C57Bl6 and 1.56% SJL). These mice were then crossed with 129/OlaHsd mice (Harlan France Sarl) to obtain $Cr^{+/-}$ and $Cr^{+/-}$ Tg^{+} mice that were then crossed between each other to obtain littermates $Cr^{+/+}$, $Cr^{-/-}$, and $Cr^{-/-}$ Tg^{+} mice with a genetic background theoretically consisting of 49.22% C57Bl6, 0.78% SJL, and 50% 129.

All animals were housed in groups of two to five in clear plastic cages and maintained in a temperature- and humidity-controlled room on a 12 h light-dark schedule with food and water provided ad libidum. The study was approved by the Institutional Ethical Committee of the School of Medicine, Université Libre de Bruxelles, Belgium.

In situ hybridization

Mice were killed by neck dislocation. Their brains were removed and frozen in 2-methylbutane cooled by dry ice. Parasagittal sections (15 μm) were mounted onto slides coated with poly-L-lysine and stored at –20 C. Sections were fixed in a buffered 4% paraformaldehyde solution for 30 min, rinsed in PBS 0.1 M, dehydrated, and dipped for 3 min in chloroform. After air drying, the sections were incubated overnight at 42°C with 0.35×10^{6} c.p.m. per section of ^{35}S-labeled probe diluted in hybridization buffer, which consisted of 50% formamide, 4× standard saline citrate (SSC, where 1× SSC is 0.15 M NaCl, 0.015 M sodium citrate, pH 7.4), 1 × Denhardt's solution (0.02% each of polyvinylpyrrolidone, bovine serum albumin, ficoll), 1% sarcosyl, 0.02 M sodium phosphate at pH 7.4, 10% dextran sulfate, yeast tRNA at 500 μg/ml, salmon sperm DNA at 100 μg/ml, and 60 mM dithiothreitol (Sigma, St. Louis, MO). After hybridization, the sections were rinsed for 4 × 15 min in 1× SSC at 55°C, dehydrated, and covered with Kodak (Rochester, NY) Bio Max MR film for 10–12 days, and then dipped in Kodak NTB3 emulsion. Slides were exposed for 6 wk, developed, fixed, and counterstained with hematoxylin before being examined in bright- and dark-field illumination (10, 16).

The calretinin probe Cr (5′-CATGCCAGAACCCTTCCTTGCCTTCTCCAGCTCCT GGAAGAAG-3′) corresponds to bases 198-240 of the *Mus musculus* calbindin 2 (= calretinin) cDNA sequence (17). Oligonucleotide was labeled with α-^{35}S dATP (DuPont-NEN) at 3′ end by terminal DNA deoxynucleotidylexotransferase (Gibco, Gaithersburg, MD) and purified with a

nucleic acid purification cartridge (ProbeQuant G-50 micro columns, Amersham Biosciences, Buckinghamshire, UK).

Electrophoresis and immunoblotting

Cerebellum from WT and $Cr^{-/-}$ were homogenized in lysis buffer (10 µl/mg of tissue) (M-PER; Pierce, Rockford, IL) containing a protease inhibitor mixture (Complete; Roche Molecular Biochemicals, Vilvorde, Belgium). Equal amounts of protein (40, 100, or 250 µg for the densitometrical analysis) were denatured in 2× Laemmli buffer at 100°C for 5 min. Proteins were then separated on an SDS-PAGE and transferred to supported nitrocellulose (Bio-Rad, Hercules, CA). The membrane was blocked with 5% BSA and 0.1% Tween 20 in PBS buffer and then incubated with the anti-calretinin (1:10,000; Swant, Bellinzona, Switzerland), anti-$GABA_A$-α6 (1:2500; Chemicon International, Temecula, CA), or anti-actin (1:2000; Sigma) antibodies overnight at 4°C. After washing, the membrane was incubated with the HRP-labeled secondary antibody (anti-rabbit IgG; NEN, Boston, MA) at a concentration of 0.1 µg/ml for 60 min at room temperature. Immunoreactive bands were visualized by chemiluminescent ECL Plus Western blotting reagents (Amersham Biosciences). For the densitometrical analysis, the bands on the ECL hyperfilm (Amersham Biosciences) corresponding to calretinin, $GABA_A$-α6, and actin were scanned and quantified using the public domain NIH Image β4.0.2 program (National Institutes of Health, Bethesda, MD). The ratio between either calretinin or $GABA_A$-α6 and actin was used for normalization of the samples and was considered as 100% in the WT cerebellum.

Immunocytochemistry

Animals were anesthetized by i.p. injection of sodium pentobarbital (60 mg/kg) and transcardially perfused with 0.9% saline followed by 0.1 M phosphate-buffered 4% paraformaldehyde. The brain was dissected out, cryoprotected in 30% sucrose, and sectioned in the parasagittal plane. Sections were either single labeled using an anti-calretinin antiserum or double labeled with a combination of anti-GluR2/3 and anti-calretinin antisera. Single labeling: sections were incubated 1 h with 10% normal horse serum (Hormonologie Laboratoire, Marloie, Belgium) and 0.1% Triton X-100 in PBS. Sections were then incubated 36 h at 4°C with a polyclonal anti-calretinin antiserum (1/1000; Swant) in PBS and, successively with biotinylated donkey anti-rabbit IgG (H^+L) (1/200; Jackson Laboratories, West Grove, PA) and ABC complex (Elite ABC kit; Vector Laboratories, Burlingame, CA). The peroxydase activity was revealed by diaminobenzidine in the presence of hydrogen peroxide. A two-step protocol was used for double labeling since antisera were made in the same species. First, we performed and revealed the GluR2/3 staining: sections were incubated 1 h with 10% normal horse serum and 0.1% Triton X-100 in PBS. Sections were then successively incubated 36 h at 4°C with a rabbit polyclonal anti-GluR2/3 antiserum (1/75, Chemicon, Temecula, CA) diluted in PBS and 30 min with a biotinylated donckey anti-rabbit IgG (H^+L) (1/200). Amplification and visualization of the GluR2/3 signal was achieved by incubation with ABC complex (Elite ABC kit; Vector) and Alexa Fluor 488 tyramide. Sections were then examined on a confocal microscope (MRC 1024, Bio-Rad, Hertfordshire, UK) fitted on an inverted microscope (Axiovert 100, Zeiss, Oberkochen, Germany) equipped with a Plan-Neofluar ×40/1.3 oil immersion objective (Zeiss). The sections were then used for a second labeling with the polyclonal anti-calretinin antiserum (1/1000) using the technique described above. Controls included omission of the calretinin primary antibody on a WT mouse or use of this antibody on a $Cr^{-/-}$ mouse. The precise localization of the UBCs was

designated on the calretinin-labeled section by superimposing it on a scale drawing of the GluR2/3 labeling (Fig. 2*J*, 2*L*).

Single-unit recording in alert mice

Mice aged 10–13 months were prepared for chronic recording of neuronal activity in the cerebellum (10). A posterior craniotomy was performed in mice anaesthetized with xylido-dihydrothiazin (Rompun, Bayer, 10 mg/kg) and ketamine (Ketalar, Pfizer, 100 mg/kg). An acrylic recording chamber was constructed around the craniostomy, covered by a thin layer of bone wax (ethicon) before the recording session, and a silver reference electrode was placed on the surface of the parietal cortex. The mice were allowed to recover from anesthesia for 24 h, after which they were immobilized for the experimental session. Data recorded while the animal was presenting orofacial movement were discarded. Recordings were performed by optimal positioning of the glass micropipette (1.5–5 MΩ of impedance) in order to record simultaneously simple and complex spikes (12). The duration of complex spike was defined as the time between the beginning of the first depolarization and the end of the last secondary spike. Secondary spikes were counted as long as their amplitude reached at least two times the maximum amplitude of the background signal. To record the pause in simple spike firing, we averaged the simple spike during a 100 ms epoch (with a pretrigger time of 10 ms) triggered by the spontaneous occurrence of a complex spike. All recordings were performed with an amplification of 1000 and a bandwidth of 0.01–10 KHz. The recorded data were digitalized continuously at 10 KHz. Off-line analysis was performed using the Spike 2 CED software. Local field potentials were analyzed by the wave-triggered averaging technique (18). Negative peaks of the LFPO were detected, and equal windows around that point (50 ms before and 50 ms after) were extracted and averaged. These averaged oscillation sequences were quantified by fast-Fourier-transform algorithm. An oscillation index was computed by dividing the maximum amplitude of the power spectrum peak by the total area of the power spectrum (12).

Patch-clamp recordings in brain slices

Cerebellar granule cells were recorded in acute cerebellar slices obtained from 15- to 31-day-old mice. Slice preparations were performed as described previously (11, 19). Current-clamp recordings were taken from granule cells in the internal granular layer using an EPC-8 amplifier (Heka Elektronik, Lambrecht/Pfalz, Germany) in the fast current clamp mode. The perforated patch configuration of the patch-clamp technique (20) was used to maintain the endogenous Ca^{2+} buffers. The pipette solution contained the following (in mM): 80 K_2SO_4, 10 NaCl, 15 glucose, and 5 HEPES, pH adjusted at 7.2 with KOH, and 100 µg/ml nystatin. The extracellular solution contained the following (in mM): 120 NaCl, 2 KCl, 2 $CaCl_2$, 1.19 $MgSO_4$, 26 $NaHCO_3$, 1.18 KH_2PO_4, and 11 glucose equilibrated with 95% O_2/5% CO_2, pH 7.4. Access resistance was monitored to ensure that voltage attenuation in current-clamp mode was always <10%. Intrinsic excitability was investigated by setting resting membrane potential at –80 mV and injecting 1 s steps of depolarizing current (2–30 pA in 2 pA increments), and action potential frequency was measured. Passive cellular parameters were extracted in voltage clamp by analyzing current relaxation induced by a 10 mV step change from a holding potential of –70 mV as described previously (21).

Motor coordination analysis

We performed the runway test in which mice have to run along an elevated runway with low obstacles intended to impede their progress. The runway was 100 cm long and 1.2 or 1.8 cm in width, and obstacles had 0.8 and 0.5 cm diameters, respectively (see Results). The number of slips was counted on one side. Mice were given four trials per day for 5 consecutive days.

Statistics

Results are expressed as mean ± SE After confirming the normal distribution of the data using a Kolmogorov-Smirnov test, comparisons among groups were made using one- or two-way ANOVA and Bonferroni's post hoc test.

RESULTS

Cr-rescue mouse line generation and characterization of granule cell-specific expression of calretinin

To determine to which extent the absence of calretinin in granule cells contributes to the cerebellar dysfunction in $Cr^{-/-}$ mice, we generated Cr-rescue mice harboring a specific rescue of calretinin expression in these neurons. To promote a cerebellar granule cell-specific expression of calretinin, we used the promoter function of the $GABA_A$-α6. It has been reported that a 7.2 kbp mouse genomic fragment containing 5′-upstream sequence and exons 1-8 of the $GABA_A$-α6 is capable of directing selective expression of a transgene in cerebellar granule cells (15). According to this report, we constructed the calretinin transgene that consisted of the truncated $GABA_A$-α6, an IRES, the calretinin encoding cDNA, and the SV40polyA in this order: pmα6-IRES-calretinin-polyA (Fig. 1*A*). Nine founder lines were generated following microinjection of the transgene. The transgenic founders were crossed as described in Materials and Methods to obtain F3 $Cr^{-/-}$ Tg^{+} (Cr-rescue), F3 $Cr^{-/-}$ Tg^{-} (knockout) and F3 $Cr^{+/+}$ Tg^{-} (WT) mice. Two founders bred poorly and never produced F1 transgenic pups. The seven other lines were analyzed by in situ hybridization, immunohistochemistry, and immunoblotting.

In situ hybridization using a radiolabeled oligonucleotide probe revealed calretinin mRNA expression in the brain of five out the seven transgenic lines, whereas no calretinin mRNA was detected in the remaining two. In the five lines reexpressing calretinin mRNA, a similar distribution was observed with a high to very high level of expression detected in the cerebellum (Fig. 1*Bc–g*). Note that this cerebellar calretinin mRNA expression is much higher in these transgenic animals than in the cerebellum of WT mice (Fig. 1*Ba*). In all but one of these five lines, this calretinin mRNA expression is absolutely restricted to the cerebellum. In one lineage, an additional but slight expression in the pontine nuclei and occipital/retrosplenial cortex was also found (Fig. 1*Bc*). Furthermore, in these five lines, at the microscopical level, silver grains were confined to the granular layer and were never observed in Purkinje cells or molecular layers (Fig. 1*Bh–j*), confirming the calretinin mRNA reexpression in granule cells. As previously reported (10), WT mice exhibited a widespread expression pattern, whereas no calretinin mRNA expression was detected in the brain of $Cr^{-/-}$ mice (Fig. 1*Bb*).

Expression at the protein level and cell type specificity were investigated by immunohistochemistry in parasagittal brain sections. Calretinin immunoreactivity was

distributed throughout the brain in WT mice, including the cerebellar granule cells and parallel fibers in the molecular layer. As described previously, no labeling was observed in the brain of $Cr^{-/-}$ mice except a paradoxical calretinin immunoreactivity, which corresponds to calbindin-D28k, in Purkinje cells (10).

In Cr-rescue mice, calretinin immunoreactivity was only detected in granule cells of the cerebellar cortex, including in the line showing a low level of calretinin mRNA expression in pontine nuclei. In three out of the five lineages, the pattern of calretinin immunoreactivity was very similar to the WT (Fig. 2*A*) with an equivalent density of calretinin-immunoreactive granule cells (Fig. 2*C*, 2*D*, 2*F*). Conversely, the two other lineages, presented a mosaic expression detected similarly in all lobules (Fig. 2*G*, 2*H*), with calretinin-immunoreactive granule cells intermingled with negative granule cells. Note that in all five lineages of Cr-rescue mice, the paradoxical calretinin-like immunoreactivity detected in Purkinje cells persists as in $Cr^{-/-}$ mice. In WT mice, calretinin is not only expressed in the granule cells but also in UBCs and Lugaro cells. UBCs, mainly restricted to the vestibulocerebellum (22), are large and easily recognizable calretinin-positive interneurons of the granule cells layer. To determine whether calretinin would have been also re-expressed in UBCs of our Cr-rescue mice, we performed a double immunodetection of calretinin and glutamate receptor subunits GluR2/3, which are expressed in UBCs (23) and Purkinje cells. As expected, UBCs were GluR2/3-positive and calretinin-positive in WT mice and GluR2/3-positive and calretinin-negative in $Cr^{-/-}$ mice (Fig. 2*I*, 2*J*). In the different lineages of Cr-rescue mice, all UBCs were also calretinin-negative (Fig. 2*K*, 2*L*). We also measured and compared the mean area of WT UBCs (305.7±81.3 μm^2, n=54) and granule cells (91.5±18.9 μm^2, n=52) to that of calretinin-positive cells located in the vestibulocerebellum of Cr-rescue mice (86.4±16.9 μm^2, n=234). This latter was similar to the area of granule cells in WT mice (P>0.05) and highly different from that of UBCs (P<0.001, one-way ANOVA). All these results demonstrated that calretinin expression was not restored in UBCs of Cr-rescue mice. Calretinin is the only known marker for the detection of Lugaro cells (24), and no other antibody that specifically labels Lugaro cell bodies in mouse cerebellum is reported in the literature. Nevertheless, in the cerebellar cortex of these mice, we never observed calretinin-immunoreactive cells that present characteristics of Lugaro cells in WT (Fig. 2*E*), namely, ovoid somata lying in the upper granular layer, with long dendrites running in the parasagittal plane below and between the Purkinje cell bodies (24).

To ensure that the full-length calretinin protein was expressed in the cerebellum of Cr-rescue mice and to semiquantitatively evaluate the level of calretinin restoration, we performed immunoblotting on homogenates from WT, $Cr^{-/-}$, $Cr^{+/-}$, and the five different Cr-rescue mice. As described previously (10), in cerebellum homogenates, using the anti-calretinin antibody, a band at 29 kDa corresponding to the calretinin molecular weight was observed in WT and $Cr^{+/-}$ mice, whereas a band at 27 kDa that corresponds to calbindin was detected in $Cr^{-/-}$ mice (Fig. 3*C*). In the five lineages of Cr-rescue mice, we observed both the 29 kDa band corresponding to calretinin and the 27 kDa band corresponding to calbindin. No bands were observed in homogenates taken from the rest of the brain. In all these Cr-rescue mice, full-length calretinin was expressed at lower levels than endogenous calretinin (Fig. 3*A*). We estimated that calretinin was ~6–10% of the WT level in three transgenic lines and 1–2% of the WT level in the two other transgenic lines, whereas, as expected, it was at ~50% of the WT in $Cr^{+/-}$ mice (Fig. 3*C*). No calretinin was detected in homogenates selectively prepared from the pontine nuclei region in the line presenting a slight ectopic calretinin mRNA expression in this region (Fig. 3*B*).

On the basis of these results, we decided to further study the three lines of Cr-rescue mice that expressed the higher level of calretinin in the cerebellum and that also exhibit a homogeneous labeling in all granule cells. Because we directed the expression of calretinin in granule cells by using the promoter function of a fragment of $GABA_A$-α6, we checked by Western blotting for the normal expression of the endogenous $GABA_A$ receptor α6 subunit in WT, $Cr^{-/-}$, and these three different lines of Cr-rescue mice. For this immunoblotting, we used an antibody directed against the N-terminal sequence of the $GABA_A$ receptor α6 subunit and did not observe modification in the expression of this receptor in the Cr-rescue mice as compared with the WT or $Cr^{-/-}$ mice (Fig. 3*D*). Note that we never detected any additional band corresponding to the truncated form of the $GABA_A$ receptor α6 subunit probably indicating that the truncated protein is rapidly degraded. This had already been suggested by other authors using the same promoter (25, 26).

Purkinje cell firing and granule cell excitability

Since $Cr^{-/-}$ mice exhibited a dramatic alteration in Purkinje cell firing in vivo (10), the firing behavior of 552 identified Purkinje cells was analyzed in 10- to 12-month-old WT (*n*=78 cells in 4 animals), $Cr^{-/-}$ (*n*=150 cells in 9 animals), and Cr-rescue (*n*=324 cells in 15 animals) alert mice by single unit recording. As previously reported (10), the mean spontaneous simple spike firing rate was significantly enhanced in $Cr^{-/-}$ mice as compared with age-matched WT mice (Fig. 4*A*), whereas the complex spike firing rate was not statistically different (Fig. 4*B*). In the three lines of Cr-rescue mice, the simple spike firing rate was significantly lower than in $Cr^{-/-}$ mice and was restored to values not significantly different from WT (Fig. 4*A*). Note that in $Cr^{-/-}$ mice, as previously showed for calbindin-deficient ($Cb^{-/-}$) or $Cb^{-/-}$ $Cr^{-/-}$ double knockout mice (12), the increase in simple spike firing rate was much higher in Purkinje cells recorded during local field potential oscillation (LFPO) (111.7±33.7 Hz, *n*=17) than in Purkinje cells recorded in the absence of LFPO (59.7±25.3 Hz, *n*=133) ($P<0.001$). The durations of the complex spike and of the transient pause in simple spike firing following a complex spike were significantly reduced in $Cr^{-/-}$ mice as compared with the WT (Fig. 4*C*, 4*D*). As for the simple spike firing rate, both durations were completely and significantly restored to WT values in the three different lines of Cr-rescue mice (Fig. 4*C*, 4*D*).

A spontaneous high-frequency LFPO has been recently described in the cerebellum of $Cr^{-/-}$ mice and is absent in the cerebellum of WT mice (12). Therefore, we specifically and blindly looked for this oscillation in a series of 14 mice (6 Cr-rescue, 3 $Cr^{-/-}$, and 5 WT mice). All $Cr^{-/-}$ mice presented episodes of spontaneous LFPO (Fig. 4*E*), with frequency of 162 ± 48 Hz and an oscillation index of 6.4 ± 4.7. Conversely, neither WT nor Cr-rescue mice presented episodes of LFPO (Fig. 4*F*).

Intrinsic granule cell excitability was investigated on granule cells in brain slices using the perforated patch configuration of the patch-clamp technique and in current-clamp recordings. Active cell membrane properties were evaluated by measuring the voltage response while injecting steps of depolarizing current of increasing intensities in the granule cell soma. After reaching the threshold, fast regular repetitive spiking was obtained and action potential frequency increased with the intensity of the injected current. The average frequency was measured over the entire duration of current injection (1 s) and was used to construct current-frequency plots. At low current intensities, the current-frequency plots were interpolated with a straight line. Because the threshold current and maximal frequency varied substantially from cell

to cell, the evaluation of the slope factor of the linear part of current-frequency plots was used as a normalized measure of excitability. Using such analysis, we observed that the mean slope of the current-frequency plots for one line of rescued transgenic $Cr^{-/-}$ mice (4.8±0.6 Hz/pA, n=5) was equivalent to the one reported for WT mice (4.8±0.2 Hz/pA) (11). Moreover, this value is also very similar to the mean slope obtained in calretinin-deficient granule cells that have been loaded with an exogenous fast buffer, BAPTA, through the patch pipette (4.4±0.4 Hz/pA) (11). All these slope values were lower than the one recorded from $Cr^{-/-}$ mice (6.6±0.7 Hz/pA) (11). These data indicated that the excitability of $Cr^{-/-}$ granule cells is similarly restored by loading an exogenous Ca^{2+} buffer or by the reexpression of genuine calretinin in transgenic mice.

Motor coordination analysis

Previous work has revealed impaired motor coordination in $Cr^{-/-}$ mice, mostly in aged mice (10). To test whether the specific rescue of calretinin expression in granule cells and the restoration of a normal Purkinje cell firing pattern result in a normal motor behavior, we examined motor coordination of these Cr-rescue mice by using the runway test. However, conversely to data previously obtained on a mixed C57Bl6 × 129 background (10), analysis of $Cr^{-/-}$ and WT mice obtained in the present study on an almost pure C57Bl6 background (see Materials and Methods) surprisingly failed to reveal any difference between both genotypes (Fig. 5*A*). As it was established that behavior, including motor coordination, could be influenced by strain differences (27), we produced WT, $Cr^{+/-}$, and $Cr^{-/-}$ on the original C57Bl6 × 129 background. As expected (10), 12-month-old $Cr^{-/-}$ mice on this original background showed motor coordination impairment in the runway test as compared with WT mice (P<0.0001), while $Cr^{+/-}$ mice exhibited a normal motor coordination (P>0.05) (Fig. 5*B*). Hence, we produced littermates WT, $Cr^{-/-}$, and Cr-rescue mice on almost the original genetic background (see Materials and Methods). To discriminate $Cr^{-/-}$ from WT mice at the younger age of 3 months, we decreased the width of the runway (18 mm in the original test to 12 mm). In this condition, Cr-rescue and WT mice made significantly fewer errors than $Cr^{-/-}$ mice (P<0.05), while no significant differences appeared between WT and Cr-rescue mice (P>0.05) (two-way repeated ANOVA) (Fig. 5*C*).

DISCUSSION

In this report, we successfully produced lines of transgenic mice, rescuing specifically the expression of calretinin in granule cells of the cerebellum of $Cr^{-/-}$ mice. Using this model, we have shown that this selective rescue restored 1) a WT Purkinje cell firing behavior leading to the absence of oscillation, 2) a normal neuronal excitability of granule cells in slices, and 3) a normal motor coordination as compared with the alterations detected in $Cr^{-/-}$ mice (10, 11).

Calretinin is a cytoplasmic protein belonging to the large family of EF-hand calcium binding proteins (28) that play a crucial role in the complex regulatory system of calcium homeostasis. In the cerebellum, calretinin is the major calcium binding protein known to be expressed in granule cells but is also present in two other neuronal subtypes of the granule cell layer: UBCs and Lugaro cells (8, 9). Both are more intensely stained with anti-calretinin antisera than granule cells, suggesting that they contain higher calretinin concentrations. Moreover, it was also detected in subsets of mossy and climbing fibers (13, 14), major afferents to granule and Purkinje cells, respectively. Because calretinin is not expressed in Purkinje cells, their firing alterations observed in $Cr^{-/-}$ mice (10) have to be an indirect consequence of the mutation. Since

granule cells excite Purkinje cells through parallel fibers, the increased Purkinje cell firing rate could be explained by an increased granule cell to Purkinje cell transmission. In line with this hypothesis, an increased granule cell excitability has been recently demonstrated in slices (11). However, an increased excitability of Lugaro cells induced by the calretinin deficiency could also lead to an increased activity at the level of Purkinje cells. Indeed, Lugaro cells are believed to exert a disinhibitory influence on Purkinje cells via a glycinergic inhibition of Golgi cells (24). Finally, an enhancement of Purkinje cells firing could also result from an increased feed-forward excitation by UBCs through activation of granule cells (29) or from an increased synaptic transmission due to the absence of calretinin in subsets of mossy or climbing fibers.

Although granule cells expressed calretinin in our different lineages of Cr-rescue mice, Lugaro cells or UBCs expressing calretinin were never observed and no calretinin was detected in neurons outside the cerebellum, therefore allowing us to assess for the specific involvement of calretinin in granule cells.

Interestingly, the specific rescue of calretinin in granule cells also normalized the climbing fiber response, which is altered in $Cr^{-/-}$ mice as evidenced by a decrease of the complex spike duration. This strongly suggests that this modification results from an alteration in the activity within the network of inhibitory neurons. Indeed, parallel fiber stimulation may negatively regulate the complex spike duration through activation of inhibitory interneurons of the molecular layer (30–32). An increase in granule cell excitability and simple spike firing rate, as observed in $Cr^{-/-}$ mice, could therefore induce the observed reduction in complex spike duration and, as a consequence, the reduction of the pause duration. Similar changes in complex spike and transient pause durations have been described after direct stimulation of stellate cells in vitro (32).

A very high calretinin mRNA expression was detected in the cerebellum of the Cr-rescue animals as compared with the WT expression. This could be explained by the very high cerebellar expression of the $GABA_A$ receptor α6 subunit, whose gene has been used to direct calretinin expression in granule cells, as compared with other $GABA_A$ receptor subunits (33–35). Despite the very high level of calretinin mRNA detected in the cerebellum, the amount of protein is relatively low in all Cr-rescue mice as compared with WT mice. This low translational efficacy could be explained by the design of the bicistronic construct containing an IRES. Certain coding sequences can exert a negative effect on IRES-mediated translation, and this inhibitory activity is only exerted from the first cistron (36). In our construct, this could be the case for the used fragment of the $GABA_A$-α6, therefore limiting the level of rescued calretinin to ~10% of the WT.

Despite this low level of calretinin, it was sufficient to restore normal granule cell excitability, Purkinje cell firing, and motor coordination. Note that heterozygous $Cr^{+/-}$ mice also exhibited a normal motor behavior, confirming that a full amount of calretinin in granule cells is not required for a normal cerebellar physiology. Several examples, either in rescued mice with 80-fold less protein than in WT (37) or in heterozygous mice (38, 39), illustrate that a full protein expression is not absolutely necessary for a normal phenotype. All these observations could result from functional redundancy, compensation, or both. Indeed, other calcium concentration regulating processes, still unidentified in granule cells, may either partially compensate for the absence of calretinin in $Cr^{-/-}$ mice or redundantly take part in its function in all genotypes. We previously suggested the existence of compensatory mechanisms at work in $Cr^{-/-}$ granule cells. Indeed, no

spike-frequency accommodation was recorded in these cells, while recordings with low BAPTA concentration (0.01 mM) on WT, designed to mimic the mutant, expectedly resulted in a severe spike-frequency accommodation (11). On the other hand, it could be also argued that calretinin may ensure its function with a low amount of protein if adequately localized in a submembrane compartment. Altogether, these observations suggest that studies using siRNA in the brain could lead to frustrating results since a 90% knockdown protein expression may be functionally irrelevant.

Motor coordination has been analyzed in mice generated on different backgrounds. Our first analysis of $Cr^{-/-}$ and WT mice obtained on an almost pure C57Bl6 background and challenged on a runway test surprisingly failed to reveal any differences between both genotypes. It is now clearly established that the genetic background can affect the expression of a given mutation. This was nicely illustrated recently by the near-total suppression of a severe cerebellar phenotype through transferring a null allele mutation form the inbred 129/Sv strain to the C57Bl/6J background (40). Behavior, including motor coordination, could be also influenced by strain differences, the C57Bl/6J strain being more efficient in motor coordination tests and less anxious in the elevated plus-maze test as compared with C57Bl6 × 129 mice (27, 41–43). This means that, for a given test, a subtle motor impairment, as in $Cr^{-/-}$ mice, could be revealed in C57Bl/6 × 129 and not in C57Bl/6 mice, as reported in this study. This strongly suggests that, although not available, a more refined and sensitive behavioral motor testing would be able to unmask a defect in this latter strain. On this basis, we produced all genotypes on the original C57Bl6 × 129 background. This allowed showing the motor coordination impairment of $Cr^{-/-}$ mice as previously reported (10) and the restoration of a WT motor behavior in Cr-rescue mice. Although a difference in the importance of Cr in controlling physiological and behavioral events cannot definitely be excluded, it is highly reasonable that, conversely, unidentified factors in the genetic background slightly modify the motor performance of strains and hence their sensitivity to the Cr deficiency.

The selective rescue of calretinin expression in granule cells of $Cr^{-/-}$ mice definitively proves that its control of the Purkinje cell firing only occurs through a subtle regulation of the granule cell intrinsic excitability. Consequently, by showing that the level of calretinin expression specifically in granule cells regulates their excitability, the Purkinje cell firing, and ultimately motor coordination, these results demonstrate that the fine-tuning of granule cell excitability plays a crucial role in the control of information coding and storage in the cerebellum. Moreover, they also show that, by its fine control of calcium homeostasis, calretinin in granule cells is an essential actor to provide a correct computation in the cerebellar cortex.

ACKNOWLEDGMENTS

We thank W. Wisden for the generous gift of the pmα6IRES-LacZ6 plasmid, C. Thomson for his help with $GABA_A$ receptor α6 subunit immunoblotting, L. Cuvelier and D. Houtteman for their expert assistance, J. M. Vanderwinden for help with confocal microscopy, and V. Demaertelaer for her helpful comments on statistical procedures. BB and CR were supported by FRIA (Belgium). This work was supported by FMRE (Belgium), FNRS (Belgium), Van Buuren Foundation, Action de Recherche Concertée (2002–2007), and research funds of ULB and UMH. LS, AdK, and SS were research fellow, research associate, and senior research associate, respectively, at FNRS (Belgium).

REFERENCES

1. Clapham, D. E. (1995) Calcium signaling. *Cell* **80,** 259–268

2. Usowicz, M. M., Sugimori, M., Cherksey, B., and Llinas, R. (1992) P-type calcium channels in the somata and dendrites of adult cerebellar Purkinje cells. *Neuron* **9,** 1185–1199

3. Kano, M., Rexhausen, U., Dreessen, J., and Konnerth, A. (1992) Synaptic excitation produces a long-lasting rebound potentiation of inhibitory synaptic signals in cerebellar Purkinje cells. *Nature* **356,** 601–604

4. D'Angelo, E., De Filippi, G., Rossi, P., and Taglietti, V. (1997) Synaptic activation of Ca2+ action potentials in immature rat cerebellar granule cells in situ. *J. Neurophysiol.* **78,** 1631–1642

5. Sakurai, M. (1990) Calcium is an intracellular mediator of the climbing fiber in induction of cerebellar long-term depression. *Proc. Natl. Acad. Sci. USA* **87,** 3383–3385

6. Hansel, C., Linden, D. J., and D'Angelo, E. (2001) Beyond parallel fiber LTD: the diversity of synaptic and non-synaptic plasticity in the cerebellum. *Nat. Neurosci.* **4,** 467–475

7. Ito, M. (1989) Long-term depression. *Annu. Rev. Neurosci.* **12,** 85–102

8. Marini, A. M., Strauss, K. I., and Jacobowitz, D. M. (1997) Calretinin-containing neurons in rat cerebellar granule cell cultures. *Brain Res. Bull.* **42,** 279–288

9. Resibois, A., and Rogers, J. H. (1992) Calretinin in rat brain: an immunohistochemical study. *Neuroscience* **46,** 101–134

10. Schiffmann, S. N., Cheron, G., Lohof, A., d'Alcantara, P., Meyer, M., Parmentier, M., and Schurmans, S. (1999) Impaired motor coordination and Purkinje cell excitability in mice lacking calretinin. *Proc. Natl. Acad. Sci. USA* **96,** 5257–5262

11. Gall, D., Roussel, C., Susa, I., D'Angelo, E., Rossi, P., Bearzatto, B., Galas, M. C., Blum, D., Schurmans, S., and Schiffmann, S. N. (2003) Altered neuronal excitability in cerebellar granule cells of mice lacking calretinin. *J. Neurosci.* **23,** 9320–9327

12. Cheron, G., Gall, D., Servais, L., Dan, B., Maex, R., and Schiffmann, S. N. (2004) Inactivation of calcium-binding protein genes induces 160 Hz oscillations in the cerebellar cortex of alert mice. *J. Neurosci.* **24,** 434–441

13. Fortin, M., Marchand, R., and Parent, A. (1998) Calcium-binding proteins in primate cerebellum. *Neurosci. Res.* **30,** 155–168

14. Dino, M. R., Willard, F. H., and Mugnaini, E. (1999) Distribution of unipolar brush cells and other calretinin immunoreactive components in the mammalian cerebellar cortex. *J. Neurocytol.* **28,** 99–123

15. Bahn, S., Jones, A., and Wisden, W. (1997) Directing gene expression to cerebellar granule cells using gamma-aminobutyric acid type A receptor alpha6 subunit transgenes. *Proc. Natl. Acad. Sci. USA* **94,** 9417–9421

16. Schurmans, S., Schiffmann, S. N., Gurden, H., Lemaire, M., Lipp, H. P., Schwam, V., Pochet, R., Imperato, A., Bohme, G. A., and Parmentier, M. (1997) Impaired long-term potentiation induction in dentate gyrus of calretinin-deficient mice. *Proc. Natl. Acad. Sci. USA* **94,** 10415–10420

17. Strausberg, R. L., et al. (2002) Generation and initial analysis of more than 15,000 full-length human and mouse cDNA sequences. *Proc. Natl. Acad. Sci. USA* **99,** 16899–16903

18. Steriade, M., Amzica, F., Neckelmann, D., and Timofeev, I. (1998) Spike-wave complexes and fast components of cortically generated seizures. II. Extra- and intracellular patterns. *J. Neurophysiol.* **80,** 1456–1479

19. D'Angelo, E., De Filippi, G., Rossi, P., and Taglietti, V. (1998) Ionic mechanism of electroresponsiveness in cerebellar granule cells implicates the action of a persistent sodium current. *J. Neurophysiol.* **80,** 493–503

20. Horn, R., and Marty, A. (1988) Muscarinic activation of ionic currents measured by a new whole-cell recording method. *J. Gen. Physiol.* **92,** 145–159

21. D'Angelo, E., De Filippi, G., Rossi, P., and Taglietti, V. (1995) Synaptic excitation of individual rat cerebellar granule cells in situ: evidence for the role of NMDA receptors. *J. Physiol.* **484,** 397–413

22. Dino, M. R., Willard, F. H., and Mugnaini, E. (1999) Distribution of unipolar brush cells and other calretinin immunoreactive components in the mammalian cerebellar cortex. *J. Neurocytol.* **28,** 99–123

23. Nunzi, M. G., Birnstiel, S., Bhattacharyya, B. J., Slater, N. T., and Mugnaini, E. (2001) Unipolar brush cells form a glutamatergic projection system within the mouse cerebellar cortex. *J. Comp. Neurol.* **434,** 329–341

24. Dieudonne, S., and Dumoulin, A. (2000) Serotonin-driven long-range inhibitory connections in the cerebellar cortex. *J. Neurosci.* **20,** 1837–1848

25. Jones, A., Korpi, E. R., McKernan, R. M., Pelz, R., Nusser, Z., Makela, R., Mellor, J. R., Pollard, S., Bahn, S., Stephenson, F. A., et al. (1997) Ligand-gated ion channel subunit partnerships: GABAA receptor alpha6 subunit gene inactivation inhibits delta subunit expression. *J. Neurosci.* **17,** 1350–1362

26. Yamamoto, M., Wada, N., Kitabatake, Y., Watanabe, D., Anzai, M., Yokoyama, M., Teranishi, Y., and Nakanishi, S. (2003) Reversible suppression of glutamatergic neurotransmission of cerebellar granule cells in vivo by genetically manipulated expression of tetanus neurotoxin light chain. *J. Neurosci.* **23,** 6759–6767

27. Voikar, V., Koks, S., Vasar, E., and Rauvala, H. (2001) Strain and gender differences in the behavior of mouse lines commonly used in transgenic studies. *Physiol. Behav.* **72,** 271–281

28. Persechini, A., Moncrief, N. D., and Kretsinger, R. H. (1989) The EF-hand family of calcium-modulated proteins. *Trends Neurosci.* **12,** 462–467

29. Dino, M. R., Schuerger, R. J., Liu, Y., Slater, N. T., and Mugnaini, E. (2000) Unipolar brush cell: a potential feedforward excitatory interneuron of the cerebellum. *Neuroscience* **98,** 625–636

30. Callaway, J. C., Lasser-Ross, N., and Ross, W. N. (1995) IPSPs strongly inhibit climbing fiber-activated [Ca2+]i increases in the dendrites of cerebellar Purkinje neurons. *J. Neurosci.* **15,** 2777–2787

31. Campbell, N. C., Ekerot, C. F., and Hesslow, G. (1983) Interaction between responses in Purkinje cells evoked by climbing fibre impulses and parallel fibre volleys in the cat. *J. Physiol.* **340,** 225–238

32. Midtgaard, J. (1992) Stellate cell inhibition of Purkinje cells in the turtle cerebellum in vitro. *J. Physiol.* **457,** 355–367

33. Kim, Y., and Oh, S. (2002) Changes of GABA(A) receptor binding and subunit mRNA level in rat brain by infusion of NOS inhibitor. *Brain Res.* **952,** 246–256

34. Wu, C. H., Frostholm, A., De Blas, A. L., and Rotter, A. (1995) Differential expression of GABAA/benzodiazepine receptor subunit mRNAs and ligand binding sites in mouse cerebellar neurons following in vivo ethanol administration: an autoradiographic analysis. *J. Neurochem.* **65,** 1229–1239

35. Laurie, D. J., Seeburg, P. H., and Wisden, W. (1992) The distribution of 13 GABAA receptor subunit mRNAs in the rat brain. II. Olfactory bulb and cerebellum. *J. Neurosci.* **12,** 1063–1076

36. Hennecke, M., Kwissa, M., Metzger, K., Oumard, A., Kroger, A., Schirmbeck, R., Reimann, J., and Hauser, H. (2001) Composition and arrangement of genes define the strength of IRES-driven translation in bicistronic mRNAs. *Nucleic Acids Res.* **29,** 3327–3334

37. Ichise, T., Kano, M., Hashimoto, K., Yanagihara, D., Nakao, K., Shigemoto, R., Katsuki, M., and Aiba, A. (2000) mGluR1 in cerebellar Purkinje cells essential for long-term depression, synapse elimination, and motor coordination. *Science* **288,** 1832–1835

38. Ferguson, S. M., Bazalakova, M., Savchenko, V., Tapia, J. C., Wright, J., and Blakely, R. D. (2004) Lethal impairment of cholinergic neurotransmission in hemicholinium-3-sensitive choline transporter knockout mice. *Proc. Natl. Acad. Sci. USA* **101,** 8762–8767

39. Brew, H. M., Hallows, J. L., and Tempel, B. L. (2003) Hyperexcitability and reduced low threshold potassium currents in auditory neurons of mice lacking the channel subunit Kv1.1. *J. Physiol.* **548,** 1–20

40. Bilovocky, N. A., Romito-DiGiacomo, R. R., Murcia, C. L., Maricich, S. M., and Herrup, K. (2003) Factors in the genetic background suppress the engrailed-1 cerebellar phenotype. *J. Neurosci.* **23,** 5105–5112

41. Bearzatto, B., Servais, L., Cheron, G., and Schiffmann, S. N. (2005) Age-dependence of strain determinant on mice motor coordination. *Brain Res.* **1039,** 37–42

42. Rogers, D. C., Jones, D. N., Nelson, P. R., Jones, C. M., Quilter, C. A., Robinson, T. L., and Hagan, J. J. (1999) Use of SHIRPA and discriminant analysis to characterise marked differences in the behavioural phenotype of six inbred mouse strains. *Behav. Brain Res.* **105,** 207–217

43. Homanics, G. E., Quinlan, J. J., and Firestone, L. L. (1999) Pharmacologic and behavioral responses of inbred C57BL/6J and strain 129/SvJ mouse lines. *Pharmacol. Biochem. Behav.* **63,** 21–26

Received February 2, 2005; accepted October 11, 2005.

Fig. 1

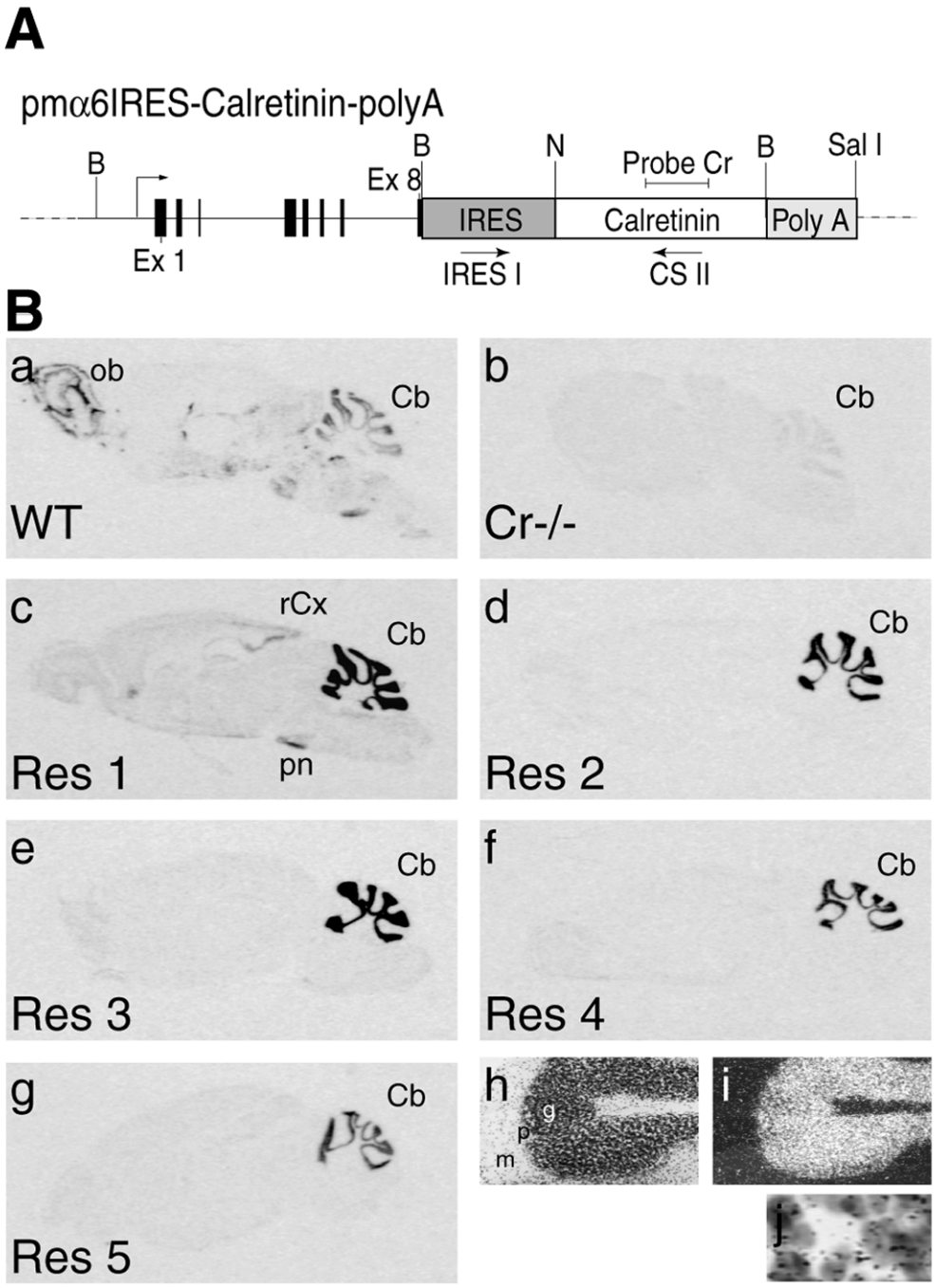

Figure 1. Generation and characterization of Cr-rescue mice. ***A*)** The calretinin encoding cDNA (calretinin) and the SV40 polyadenylation site (Poly A) were inserted downstream of a 7.2 kbp mouse genomic fragment containing 5'-upstream sequence and exons (Ex) 1-8 of the $GABA_A$-α6 gene flanked by an internal ribosome entry site (IRES). Exons of the $GABA_A$-α6 gene are shown by filled boxes. Curved arrow indicates the transcriptional start site, the IRES I, and CS II arrows indicate the position of the primers used for genotyping, "Probe Cr" indicates the position of the probe used for in situ hybridization. N, NcoI; B, BamHI. ***B*)** In situ hybridization performed on parasagittal brain sections using a radiolabeled calretinin antisense oligonucleotide probe. Calretinin mRNA is only, and strongly, detected in the cerebellum of the 5 Cr-rescue lineages (***c–g***) as compared with the widespread expression in WT mice (***a***) and the absence of expression in $Cr^{-/-}$ mice (***b***). In one lineage (***c***), a slight expression was also detected in pontine nuclei (pn) and retrosplenial cortex (rCx). At the microscopical level (***h–j***), silver grains were confined to the granular layer and were never observed in Purkinje cell or molecular layers. Bright (***h***) and darkfield (***i***) illuminations were used. ***j*)** Granule cells at high magnification. ob, olfactory bulb; Cb, cerebellum; m, molecular layer; p, Purkinje cell layer; g, granule cell layer.

Fig. 2

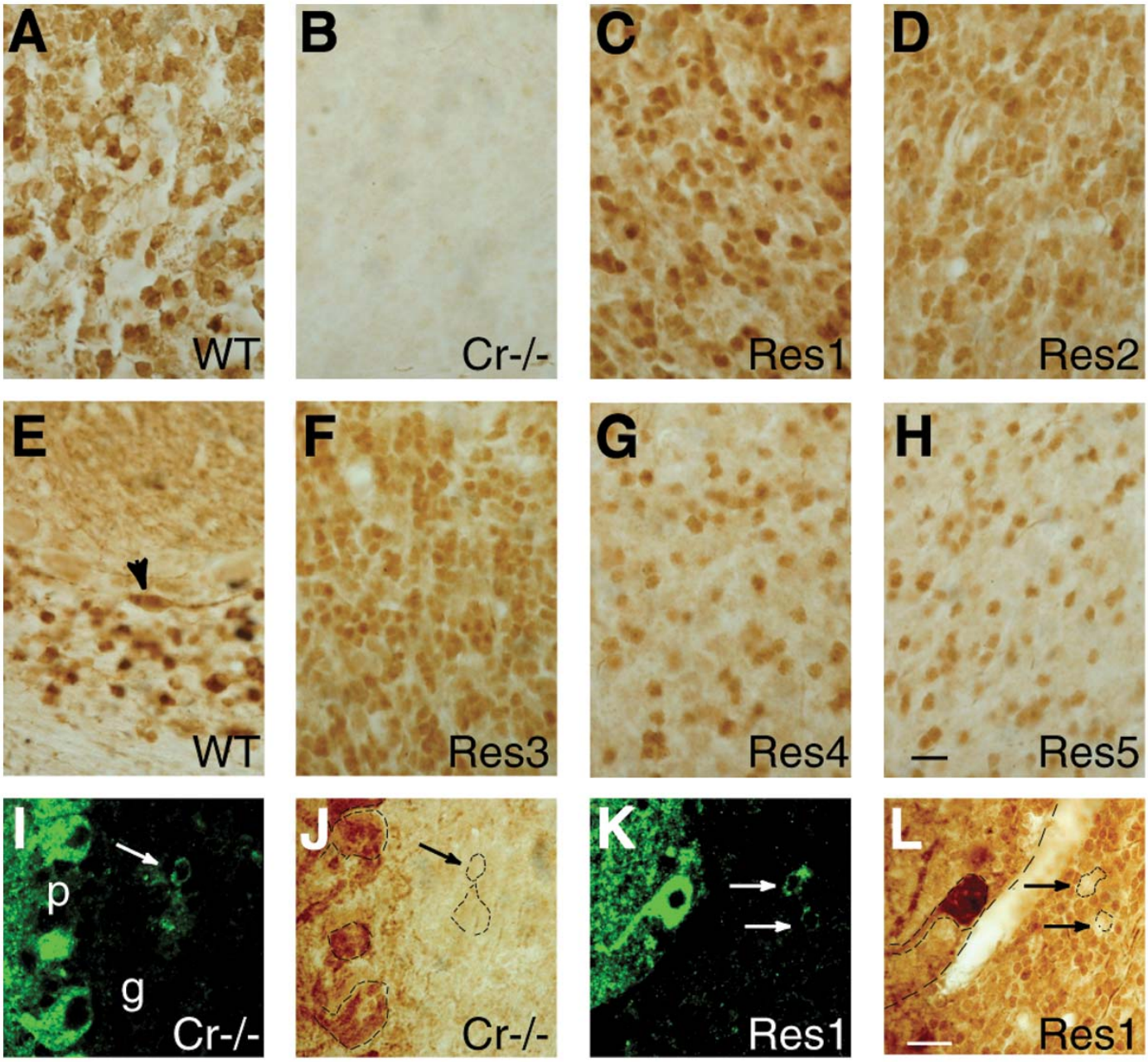

Figure 2. Calretinin-immunolabeling on parasagittal brain sections (***A–H***). In WT cerebellum, calretinin is mostly detected in granule cells (***A***) and in Lugaro cells (***E***). No labeling was observed in $Cr^{-/-}$ mice (***B***) except a paradoxical staining in Purkinje cells (***J***). Three lineages of Cr-rescue mice (***C***, ***D***, ***F***) present a pattern of calretinin-immunoreactivity in granule cells that is very similar to WT mice. The others exhibit a mosaic expression, with calretinin-immunoreactive granule cells intermingled with negative ones (***G***, ***H***). Double labeling using anti-GluR2/3 (***I***, ***K***) and anti-calretinin (***J***, ***L***) antibodies did not show calretinin expression in UBCs in $Cr^{-/-}$ (***J***) or Cr-rescue (***L***) mice. Arrows, UBCs; arrowhead, Lugaro cell; g, granular layer; p, Purkinje cell layer. Scale bars = 20μm.

Fig. 3

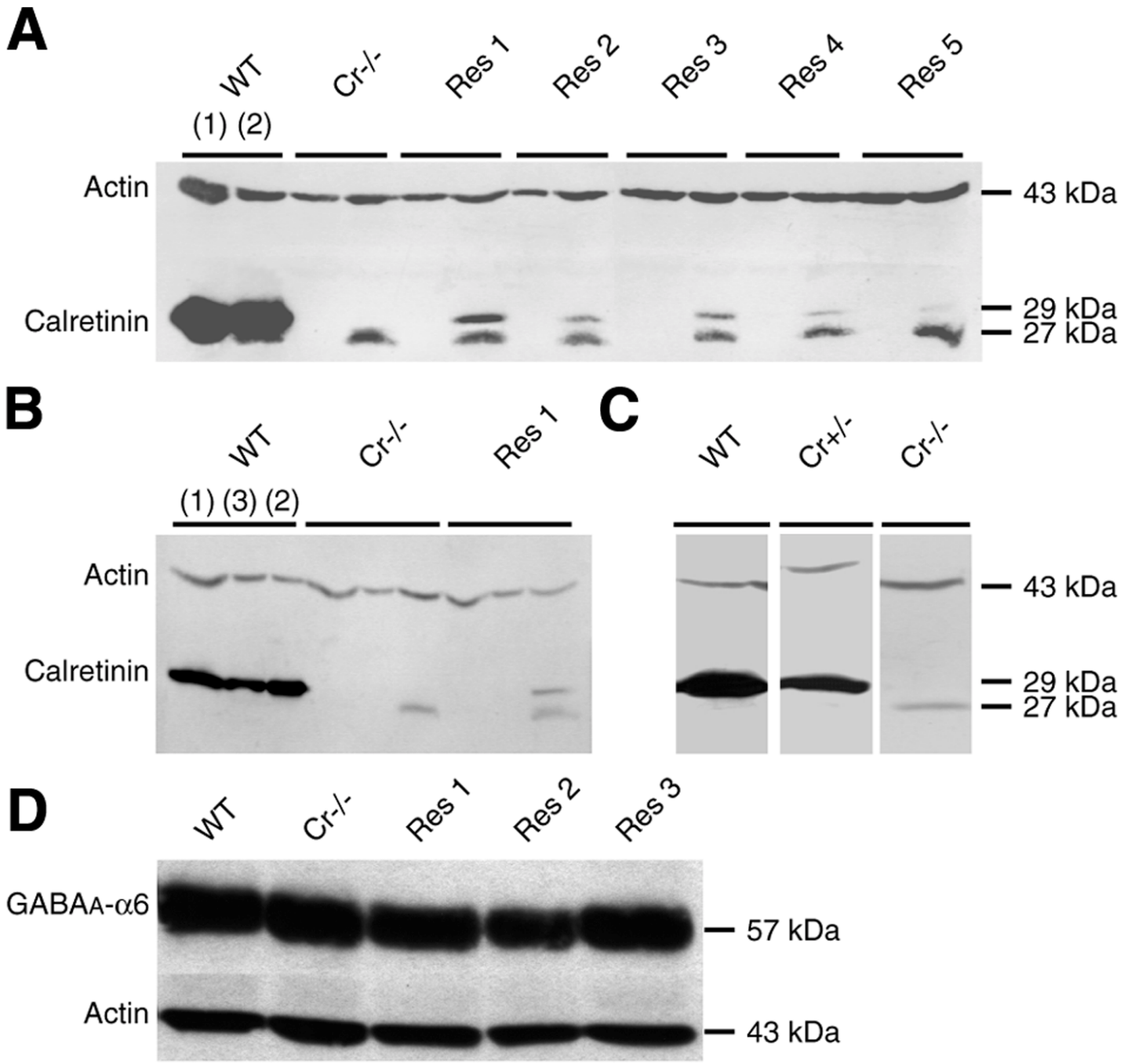

Figure 3. Western blot analysis from proteins isolated from cerebellum (lane 2) and the rest of the brain (lane 1) of WT, $Cr^{-/-}$, $Cr^{+/-}$, and Cr-rescue mice (Res 1-5) and probed with an anti-calretinin polyclonal antibody. ***A*)** In the five lines of Cr-rescue mice, a 29 kDa band corresponding to the calretinin molecular weight was detected in the cerebellum and not in the rest of the brain. A 27 kDa band corresponding to calbindin was present in the cerebellum (2) from $Cr^{-/-}$ and Cr-rescue mice. ***B*)** In the Res 1 mice presenting a slight ectopic calretinin mRNA expression in the pontine nuclei, no calretinin was detected in homogenates prepared from this region (lane 3). ***C*)** A reduced level of calretinin is observed in the cerebellum of $Cr^{+/-}$ mice as compared with WT mice. ***D*)** Proteins isolated from cerebellum of WT, $Cr^{-/-}$, and Cr-rescue mice were probed with an anti-$GABA_A$-α6 subunit receptor antibody. A 57 kDa band corresponding to the $GABA_A$-α6 subunit receptor is present in cerebellum of all mice. No modification in the expression of this receptor is detected in the Cr-rescue mice as compared with either WT or $Cr^{-/-}$ mice.

Fig. 4

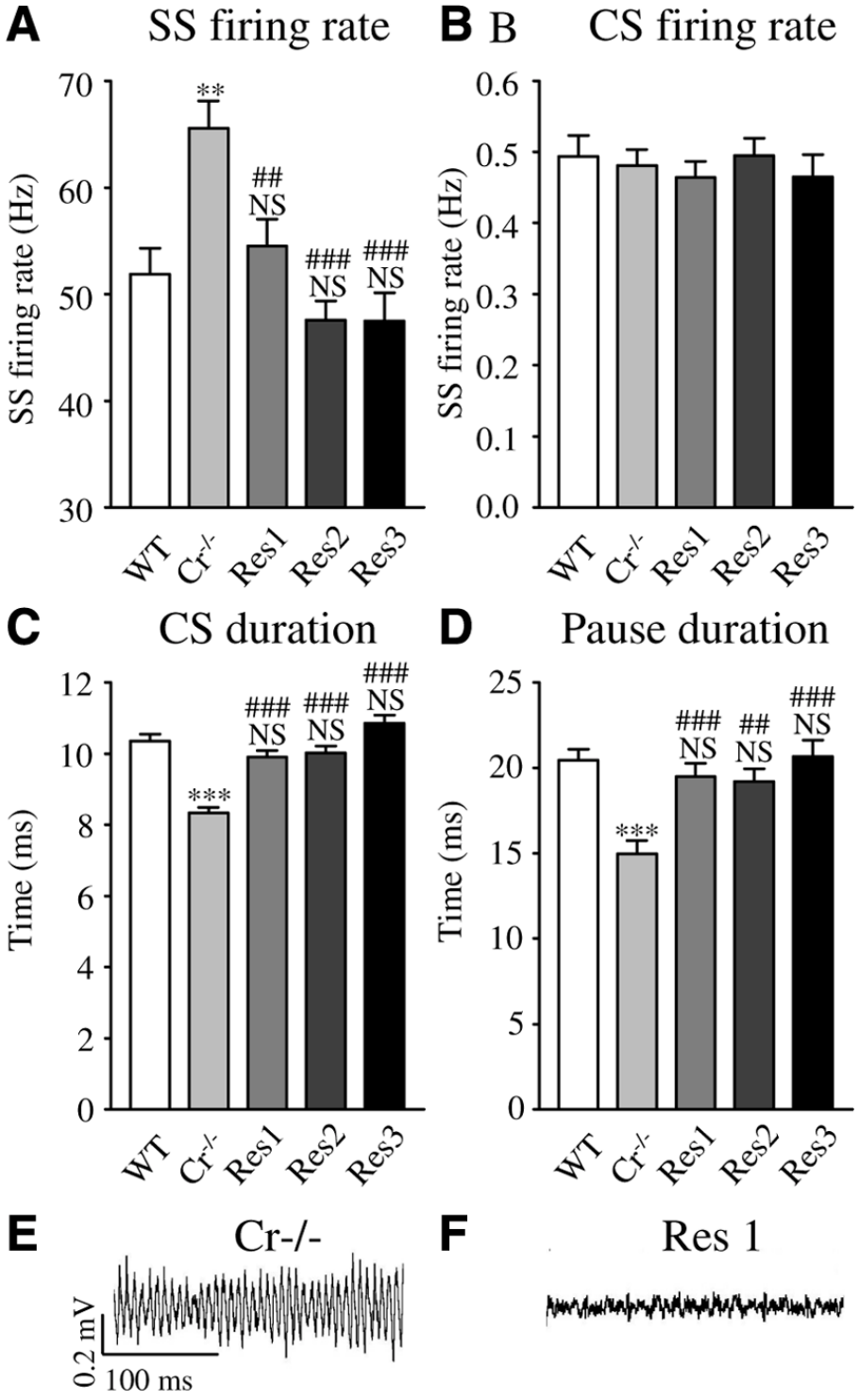

Figure 4. In vivo single-unit recordings of extracellular Purkinje cells activity in alert 10- to 12-month-old WT mice (n=78 cells), $Cr^{-/-}$ mice (n=150 cells), and Cr-rescue mice: Res1 (n=113 cells), Res2 (n=130 cells), and Res3 (n=81 cells). Analysis of spontaneous simple spike (SS) firing rate (***A***), spontaneous complex spike (CS) firing rate (***B***), CS duration (***C***), and pause duration (***D***) showed that re-expression of calretinin in Cr-rescue mice restored a wild-type Purkinje cell firing behavior. Sample records of local field potential from $Cr^{-/-}$ (***E***) and Cr-rescue (***F***) mice showed the absence of high-frequency oscillations in Cr-rescue mice. Values are mean ± SE. $^{**}P < 0.01$, $^{***}P < 0.001$, NS (nonspecific) as compared to age-matched WT; $^{\#\#}P < 0.01$, $^{\#\#\#}P < 0.001$ as compared with age-matched $Cr^{-/-}$ mice; one-way ANOVA, followed by post hoc Bonferroni's tests.

Fig. 5

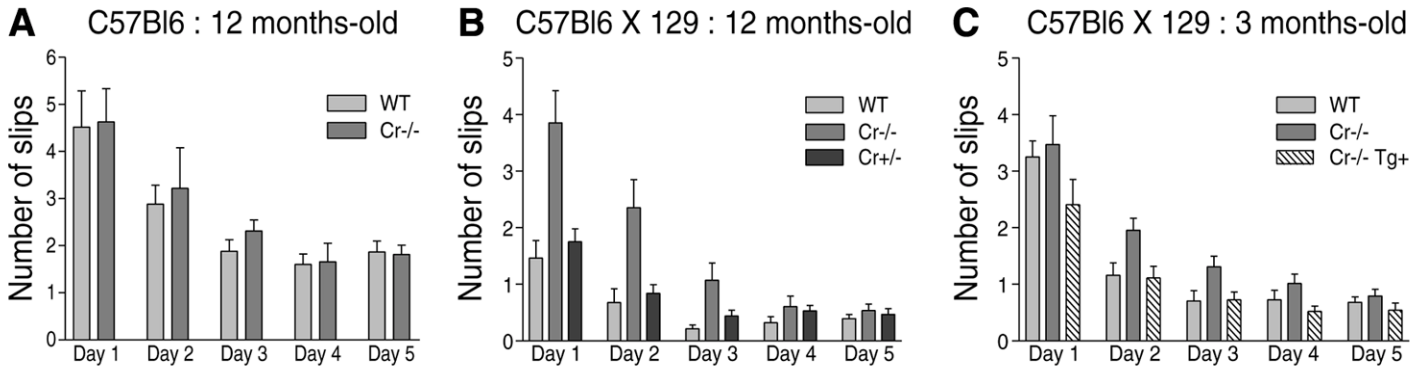

Figure 5. Motor coordination: Runway test was performed on WT, $Cr^{+/-}$, $Cr^{-/-}$, and Cr-rescue mice at different ages and different backgrounds. ***A*)** Analysis of 12-month-old C57Bl6 WT and $Cr^{-/-}$ mice (runway test on 18-mm-wide bar) did not show any difference between both genotypes. ***B*)** Twelve-month-old $Cr^{-/-}$ mice on a C57Bl6X129 background showed motor coordination impairment as compared with WT mice ($P<0.0001$); whereas $Cr^{+/-}$ mice exhibited a normal motor coordination ($P>0.05$). ***C*)** Runway test (on 12-mm-wide bar) was performed on 3-month-old WT, $Cr^{-/-}$, and Cr-rescue mice. All these mice were on a C57Bl6X129 background. This test discriminated $Cr^{-/-}$ from WT mice at the younger age of 3 months ($P<0.05$). In this condition, the Cr-rescue mice behave differently than $Cr^{-/-}$ mice ($P<0.0005$) and similarly to WT mice ($P>0.05$) (two-way repeated ANOVA).